Alcohol-Induced Protein Folding Transitions in Platelet Factor 4: The O-State†

Yingqing Yang and Kevin H. Mayo*

Department of Pharmacology and Department of Biochemistry and Molecular Biology, Jefferson Cancer Institute, Thomas Jefferson University, 10th and Locust Streets, Philadelphia, Pennsylvania 19107

Received February 26, 1993; Revised Manuscript Received May 10, 1993

ABSTRACT: Platelet factor 4 (PF4) (7800 daltons) is an anti-parallel β-sheet, α/β class protein whose tertiary structure is stabilized by the presence of two disulfide bonds. Titration of PF4 with 2-propanol or similar low molecular weight, aliphatic alcohols induces reversible protein folding transitions which are observed to be in slow exchange on the 600-MHz ^{1}H NMR time scale. Line fitting of resolved resonances assigned to ring protons of Y60, H35, H23, and αH of K50 in native and alcohol-induced states (O-states) allows derivation of folding equilibrium constants and exchange kinetics. Folding exchange rates vary between 5 and 100 s^{-1} on going from 9.8 to 3.3 M 2-propanol. Simple linear extrapolation to 0 M 2-propanol yields an O-state to N-state exchange rate of about 500 s^{-1}, i.e., millisecond time scale. At relatively high 2-propanol concentration (>9.5 M), where the O-state is predominant (>90%), NMR spectra suggest a more "unfolded" structure, while CD data indicate the preservation of considerable secondary structure. Increasing 2-propanol from 3.3 to 9.8 M, however, shifts the CD-derived fractional compositions significantly, with overall β-structure decreasing by about 20% and α-helix composition increasing by about 25%. Alcohol-jump experiments, which identify O-state long-lived NHs in the NMR spectrum of native PF4, indicate folding transition reversibility and conservation of about 15 long-lived NHs in native and O-states. Most of these NHs are assigned to residues in anti-parallel β-sheet structure. Of these 15 NHs, H/D exchange rates, although variably reduced in the O-state, are generally still long-lived compared with random coil H/D exchange. Overall, the PF4 O-state is a stable intermediate with an apparently more highly fluctuating anti-parallel β-sheet structure and a more stabilized C-terminal α-helix.

Platelet factor 4 (PF4),[1] known for its heparin binding activity (Loscalzo et al., 1985), is a platelet-specific protein of 70 amino acid residues (7800 daltons) (Deuel et al., 1977). Native human platelet factor 4, whose structure is stabilized by the presence of two disulfide bonds (Holt et al., 1986), folds with a C-terminal α-helix stacked onto an extensive anti-parallel β-sheet structural scaffold (Barker and Mayo, unpublished results) like that found for the X-ray crystal structure of bovine PF4 (St. Charles et al., 1989). In solution, native human PF4 exists in a distribution of slowly exchanging monomer–dimer–tetramer states (Mayo & Chen, 1989).

Simple alcohols at relatively low concentration have been shown to disrupt PF4 aggregate states (Barker & Mayo, 1991; Yang et al., 1993). At considerably higher concentrations, these alcohols are known both to destabilize protein folded structure (Parodi et al., 1973) and to stabilize peptide α-helix structure (Conio et al., 1970). Although this present study is focused on the effect of one of the most effective alcohols, 2-propanol, on PF4 folding, other alcohols such as methanol, ethanol, propanol, butanol, and various halogenated derivatives thereof, demonstrate similar effects at different effective concentrations (Yang et al., 1993). By using CD and ^{1}H NMR (600 MHz) methods, it is apparent that 2-propanol, and alcohols in general, shift the folding equilibrium to an intermediate, partly folded state, called the O-state. The O-state is a stable intermediate that appears in some ways to be "molten-globule"-like (Ptitsyn, 1987; Kuwajima, 1989).

The molten globule state is a commonly envoked term for prefolded structures which possess considerable secondary structure but few, if any, fixed tertiary structural contacts. This partially condensed "intermediate" state, which can usually be stabilized at equilibrium by low pH (about pH 2), low ionic strength, or elevated temperature, has been found for a number of proteins [see review by Jaenicke (1991)]. Investigation of such stable intermediates can provide useful information toward understanding protein folding. The first well-defined examples of such stable intermediates were those of α-lactalbumin and cytochrome *c* at acid pH (Dolgikh et al., 1981, 1983; Ohgushi & Wada, 1983). More detailed descriptions of those states have been provided, for example, by NMR and optical studies of α-lactalbumin (Baum et al., 1989), tryptophan synthetase β_2 (Goldberg et al., 1990), cytochrome *c* (Jeng et al., 1990), apocytochrome b_{562} (Feng et al., 1991), T4 lysozyme (Lu & Dahlquist, 1992), and heat shock protein 73 (hsp73) (Palleros et al., 1992). It has also been found that disruption of disulfide bonds in α-lactalbumin (Ewbank & Creighton, 1991), lysozyme (Radford et al., 1991), and PF4 (Mayo et al., 1992) contributes to destabilization of the native state and a shift to the molten globule state(s).

Since PF4 differs in structural character from the well-studied folding "workhorse" proteins α-lactalbumin, lysozyme, cytochromes, and RNAses which are more α-helix class proteins, this study provides an added dimension to the protein folding story by considering an example of anti-parallel β-sheet folding. Folding information on mostly β-structure proteins

† This work was supported by a grant from the National Heart, Lung, and Blood Institute (HL-43194) and benefitted from NMR facilities made available through Grant RR-04040 from the National Institutes of Health. In partial fulfillment of the Ph.D. requirements of Jefferson University for Y.Y.

* Address correspondence to this author at Department of Biochemistry, Biomedical Engineering Center, University of Minnesota, 420 Delaware St. S.E., Minneapolis, MN 55455.

[1] Abbreviations: PF4, platelet factor 4; NMR, nuclear magnetic resonance spectroscopy; 2D-NMR, two-dimensional NMR spectroscopy; NOESY, 2D-NMR nuclear Overhauser effect spectroscopy; NOE, nuclear Overhauser effect; rh, radio frequency; FID, free induction decay; CD, circular dichroism; HPLC, high-performance liquid chromatography; N-state, native state; O-state, alcohol-induced state; MT, magnetization transfer; MG, molten globule.

0006-2960/93/0432-8661$04.00/0

is rather limited. To date, the best example of folding of a mostly β-sheet protein is from work on staphylococcal nuclease (Shortle et al., 1990; Nakano & Fink, 1990). Since the time scale of protein folding is generally on the order of seconds or less, studying such partly folded transient intermediate state(s) and folding pathway(s) generally requires the use of indirect methods such as NMR proton/deutron trapping (Udgaokar & Baldwin, 1988; Roder et al., 1988; Bycroft et al., 1990), kinetic refolding of protein engineered mutants (Matouschek et al., 1990), or microcalorimetric thermodynamic dissection (Freire et al., 1992). Here, native folded and alcohol-induced O-state transitions are observed to occur on the slow ^1H NMR (600 MHz) time scale. This allows folding equilibrium constants and exchange kinetic parameters to be derived.

MATERIALS AND METHODS

Isolation of Human PF4. For PF4, outdated human platelets were obtained from the Red Cross and centrifuged at 10000*g* for 1 h to obtain platelet-poor plasma. This preparation was applied to a heparin–agarose (Sigma) column (bed volume 50 mL); the column was washed with 0.2, 0.5, 1, and 1.5 M NaCl. The fraction eluting at 1.5 M NaCl, which yielded most of the PF4 (Rucinski et al., 1979), was then desalted by dialysis (0.2% trifluoroacetic acid). The resulting solution was concentrated by lyophilization and further purified by HPLC as discussed in Mayo and Chen (1989). From about 50 units of outdated platelets, 20 mg of PF4 generally resulted.

Protein purity was checked by HPLC, gel electrophoresis, and NMR analysis. Integrity of PF4 after exposure to relatively high concentrations of 2-propanol was established by at least 5-fold dilution of PF4/60% (v/v) 2-propanol samples followed by NMR spectral analysis. Additionally, PF4 which had been exposed to 2-propanol was lyophilized and redissolved in ^2H_2O for NMR analysis. In either case, comparison to PF4 that had not been exposed to the alcohol revealed no apparent spectral changes. This can be observed in the alcohol-jump experiment presented under Results.

Protein Concentration. Protein concentration was determined according to the method of Lowry et al. (1951), and results were calculated from a standard dilution curve of human serum albumin. An alternative method used to determine PF4 concentration was that of Waddell (1956).

Nuclear Magnetic Resonance (NMR) Spectroscopy. Samples for ^1H NMR measurements had been lyophilized and redissolved in ^2H_2O and/or ^1H_2O immediately before the experiment. The final protein concentration ranged from 2 to 16 mg/mL as indicated in the text. The p^{2}H was adjusted by adding microliter increments of NaO^2H or ^2HCl to a 0.6-mL sample. All measurements were done at the p^{2}H value indicated in the text read directly from the pH meter and not adjusted for isotope effects.

^1H NMR spectra were recorded in the Fourier mode on a Bruker AMX-600 spectrometer (600 MHz for protons). The solvent deuterium signal was used as a field-frequency lock. All chemical shifts are quoted in parts per million (ppm) downfield from sodium 4,4-dimethyl-4-silapentanesulfonate (DSS). In both ^2H_2O and ^1H_2O samples, the water resonance was suppressed by direct irradiation (1 s) at the water frequency during the relaxation delay between scans. Prior to Fourier transformation, FIDs were multiplied by an exponential function to give a line broadening of 2–4 Hz.

Two-dimensional NOESY (Jeener et al., 1979; Wider et al., 1984) and HOHAHA (Bax & Davis, 1985) NMR spectra were accumulated in ^2H_2O as 512 time incremented, 1024 point spectra in the phase sensitive mode (States et al., 1982). The sweep width was 6 kHz with the carrier placed on the water resonance. Data processing was done on the Bruker X32 computer with Bruker-supplied software. FIDs were first multiplied by a Lorentzian/Gaussian transformation or shifted sine-bell function, and data sets were zero-filled to 1024 in the evolution dimension. NOESY spectra were accumulated with a mixing time of 0.2 s. 2D homonuclear magnetization transfer (HOHAHA) spectra were obtained by spin-locking with a MLEV-17 sequence with a mixing time of 60 ms. The water resonance was suppressed by direct irradiation (1 s) at the water frequency during the relaxation delay between scans in both NOESY and HOHAHA spectra, as well as during the mixing time in NOESY experiments.

Gaussian/Lorentzian Line-Shape Analysis. Resonance area integrals and half-height line widths were derived by Gaussian/Lorentzian line fitting of NMR spectra. These procedures were done on a Sun Sparc workstation with standard Gaussian/Lorentzian functions as described by Chen and Mayo (1991) or directly on the Bruker AMX 600 spectrometer X-32 computer with software supplied by Bruker. Derived areas from these fits varied from sample to sample by no more than about 10%.

Amide H/D Exchange. The exchange rates of the amide protons for deuterons of the deuterium oxide solvent were determined by measuring the time-dependent decrease of ^1H NMR line intensities as protons were replaced by deuterons. Resonance intensities were measured and calibrated relative to those of Y60 ring proton resonances. The accuracy of these measurements is estimated to be about ±20%. The experimental decay of the resonances was plotted as pseudo-first-order kinetics. In cases of multiphasic decay curves, estimates of exchange kinetics were made by measuring the initial and final slopes.

Circular Dichroism. Circular dichroic (CD) spectra were measured on a Jobin-Yvon CD-6 automatic recording spectropolarimeter coupled with a data processor. Curves were recorded digitally and fed through the data processor for signal averaging and baseline subtraction. Spectra were recorded at 30 °C in 10 mM phosphate buffer, pH 4, over 190–310 nm using a 0.1 cm path length, thermally jacketed quartz cuvette. Temperature was controlled by using a Haacke water bath. PF4 concentration was 17 μM. The scan speed was 5.0 nm/min. Spectra were signal-averaged four times, and an equally signal-averaged solvent baseline was subtracted. CD spectra were analyzed by the Provencher program for protein secondary structure prediction (Provencher & Glöckner, 1981; Provencher, 1982).

RESULTS

To follow more clearly the discussion of specific residues in PF4, backbone folds are sketched-in in Figure 1. The indicated C-terminal α-helix would be folded onto the more extensive anti-parallel β-sheet structure (St. Charles et al., 1989). The N-terminal sequence is omitted for clarity.

O-State Resonance Assignments. 2-Propanol-induced NMR spectral changes in PF4 are shown in Figure 2. In the aromatic region, native Y60, H23, and H35 resonances are observed to decrease in intensity, while new resonances increase in intensity. These resonances are labeled "N" and "O" for native state and alcohol-induced state, respectively. The appearance of separate O-state resonances which increase in intensity at the expense of N-state resonance intensity indicates the presence of N-state/O-state slow chemical exchange on

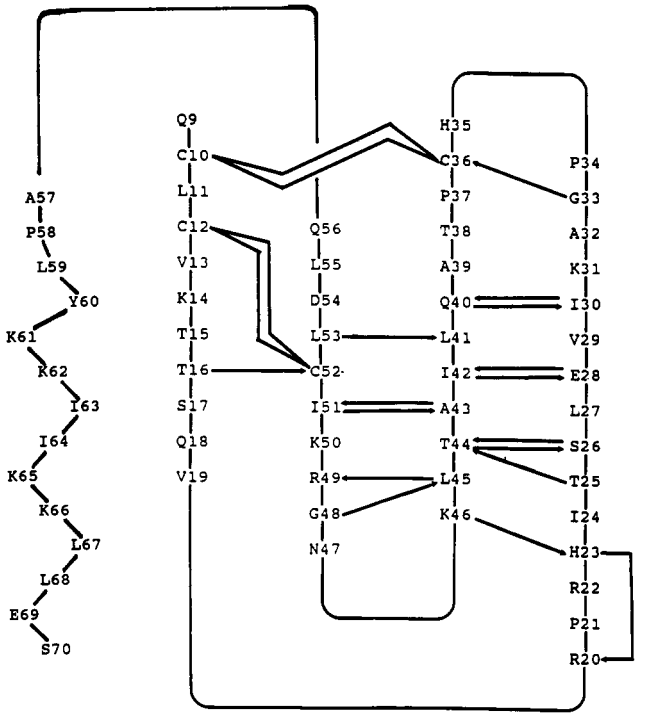

FIGURE 1: Schematic of PF4 anti-parallel β-sheet domain. A schematic representation of the PF4 backbone folding is shown. The C-terminal α-helix is actually folded onto the anti-parallel β-sheet structure (St. Charles et al., 1989). Disulfide bridges (⌒) and hydrogen bonds (H → O) are indicated.

the 600-MHz ^{1}H NMR time scale. Initial assignment of Y60 3,5 O-state resonances is obvious, while other aromatic O-state resonance assignments remain somewhat ambiguous when based solely on conventional 1D NMR spectral analysis. Assignments labeled in Figure 2 will be justified shortly.

Downfield-shifted αH resonances (Figure 2), which are structural markers for anti-parallel β-sheet folded structure in native (N-state) PF4 (Barker and Mayo, unpublished results), are also increasingly attenuated as the 2-propanol concentration is increased. In these instances, associated O-state resonances are not observed in the same spectral region. The upfield αH resonance region, however, increases significantly in intensity at the expense of these more downfield-shifted αH resonances. Therefore, these PF4 N-state anti-parallel β-sheet αH resonances are apparently highly upfield-shifted in the PF4 O-state.

The upfield methyl region, where resonances are much more convoluted, yields more simplified resonance envelopes at higher 2-propanol concentrations (Figure 3). In particular, on increasing 2-propanol concentration, two highly upfield-shifted methyl resonances become more attenuated, broaden, and shift downfield most likely to under the main methyl resonance envelope. This behavior parallels that mentioned above for aromatic and αH resonances.

Although only the effects of 2-propanol on PF4 folding are discussed here, other simple aliphatic alcohols produce the same effects. These other alcohols include methanol, ethanol, propanol, butanol, and various fluorinated derivatives of these (Yang et al., 1993). Harding et al. (1991) have also observed that at pH 2 a so-called A-state of ubiquitin is induced only in the presence of methanol. In that case, N- and A-state exchange rates fall in the NMR (500 MHz) fast-exchange regime under all conditions investigated. 2-Propanol was chosen for this study on PF4 since it is the most effective alcohol found among the above-mentioned nonfluorinated alcohols. The 2-propanol titration itself was begun at 2.8 M

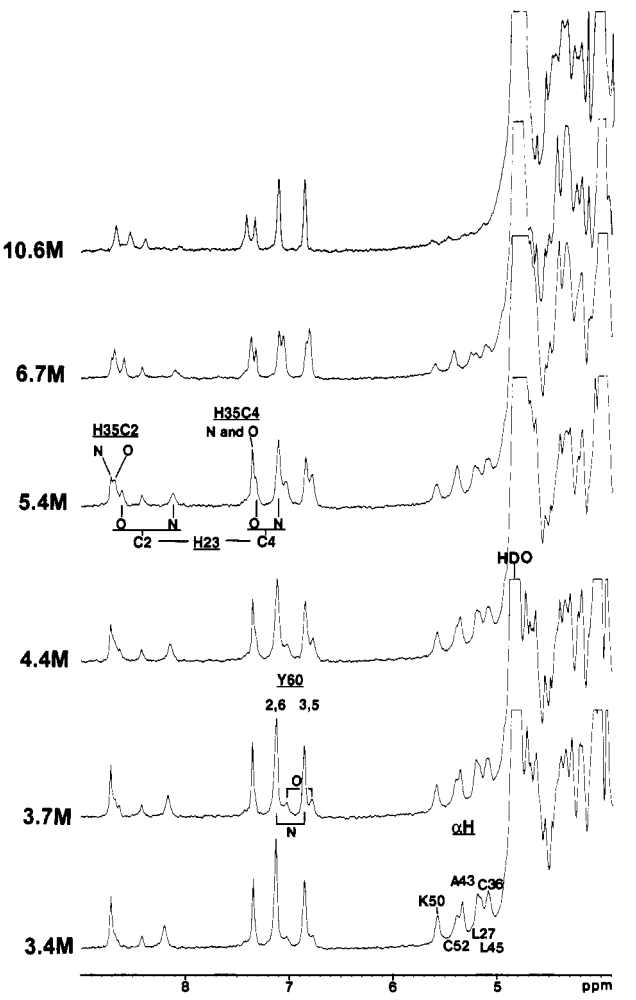

FIGURE 2: NMR spectra of PF4 in 2-propanol. 600-MHz proton NMR spectra of PF4 are shown as a function of increasing 2-propanol concentration. Lyophilized PF4 was dissolved in ^2H_2O (5 mg/mL) at pH 4, 303 K. No buffer or salt was added to the solution. Spectra shown are for aromatic and αH proton resonance regions. Not all αH resonance assignments are indicated.

due to the possibility of PF4 aggregation and aggregate-associated exchange found to exist at lower 2-propanol concentration (Yang et al., 1993). Within the 1–10 mg/mL PF4 concentration range, effects due to aggregation were not observed above about 2.4 M 2-propanol.

Resolution of state-specific resonances within the aromatic region, in combination with resonance intensity changes observed in 2-propanol titration data, makes assignment of Y60, H23, and H35 O-state resonances feasible. N-state resonances have been sequentially assigned (Barker and Mayo, unpublished results) by established 2D NMR methods (Wüthrich, 1986). For N-state aromatic and downfield αH resonances, sequence-specific assignments in the presence of low concentrations of 2-propanol could be made readily by following alcohol-induced chemical shifts in 1D NMR spectra. Figure 4 gives a 2D NMR HOHAHA contour plot of the aromatic region. The conditions of this experiment were chosen to have nearly equally populated N- and O-states. Under these conditions, Y60 2,6 and 3,5 and H35 C2 and C4 proton resonances are relatively easily assigned and grouped to N- and O-states as labeled in Figure 4.

The assignment situation for H23 O-state resonances is somewhat more complicated. pH titration of histidine resonances assists in sorting this out by allowing N- and O-state H23 and H35 C2 and C4 resonances to be grouped,

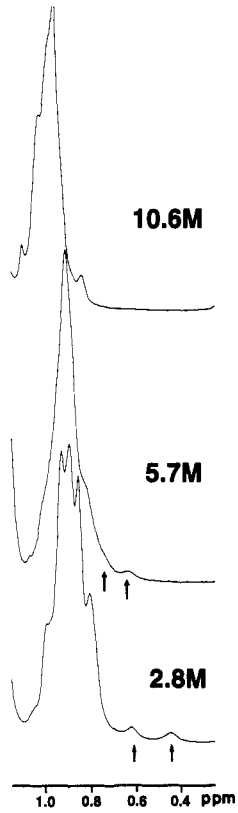

FIGURE 3: NMR spectra showing upfield aliphatic methyl region. The upfield aliphatic methyl region from NMR (600 MHz) spectra of PF4 in the presence of 2.8, 5.7, and 10.6 M 2-propanol is shown. Other solution conditions are as described in the Figure 2 legend.

respectively. Chemical shift changes of H23 and H35 N- and O-state resonances are plotted in Figure 5 as a function of the solution pH. pH values above about pH 5 were inaccessible due to limited solubility of PF4 at higher pH and low ionic strength. Titration curves for H23 in the N-state yield a pK_a value of about 3.8. This is lower than that originally reported for H23 (pK_a = 4.2–4.5) (Mayo & Chen, 1989) and may be the result of the presence of 5.7 M 2-propanol. Although H23 apparently displays only one major C2 and C4 resonance pair for each N-state and O-state (Figure 4), pH titration data suggest that multiple minor resonances (7.5–7.8 ppm), which appear primarily around the H23 pK_a, are the result of minor conformational populations. Such multiple conformation states have been previously observed for H23 (Mayo & Chen, 1989). H23 is located within a highly positively charged region of PF4 which contains a ring of lysine residues (St. Charles et al., 1989). This structural feature may provide a rational explanation for the relatively low pK_a for H23 in the N-state. Of particular note here is the observation that the pK_a for the major H23 O-state species is highly elevated relative to that in the N-state and is most likely greater than about 5 as the partial titration curve indicates. This supports the idea of an apparent structural transition from N- to O-state. N- and O-state H35 pK_a values are also clearly much greater than 5. This is consistent with a pK_a value of about 6 given for H35 in the N-state (Mayo & Chen, 1989).

The HOHAHA spectrum in Figure 4 allows C2/C4 spin system groupings to be traced out as labeled. In addition, cross-peaks apparently due to chemical exchange between/among N- and O-states are present. This is unusual. A 2D NMR NOESY spectrum of the same sample (data not shown) indicates these magnetization transfer (MT) cross-peaks as boxed-in in Figure 4. MT cross-peaks between respective

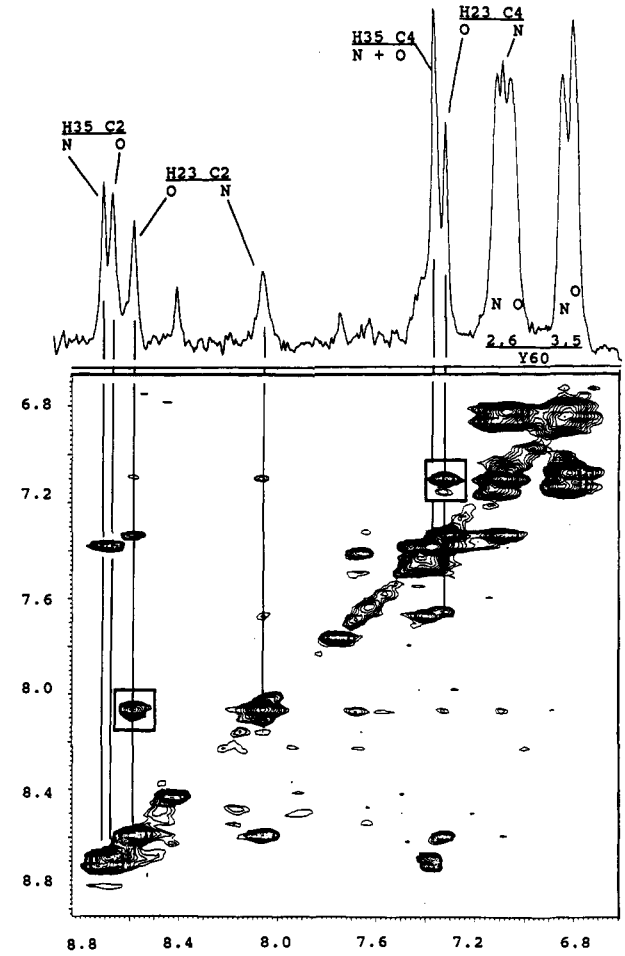

FIGURE 4: HOHAHA contour plot of PF4. A 2D NMR HOHAHA contour plot is shown for PF4 in 5.7 M 2-propanol, 303 K, pH 4. Under these solution conditions, N- and O-state populations are nearly equal. Some cross-peaks which are present in a respective NOESY spectrum are boxed-in in this figure. Resonances and cross-peaks are labeled as described in the text.

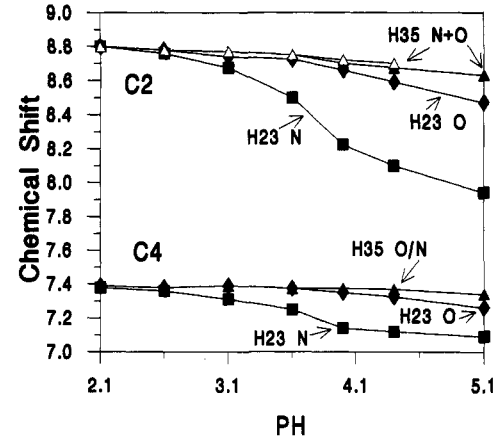

FIGURE 5: pH titration plots for H35 and H23 C2 and C4 resonances. Plots are shown of H23 and H35 C2 and C4 resonance chemical shifts as a function of solution pH (not corrected for isotope effects). The PF4 concentration was 5 mg/mL, and the 2-propanol concentration was 5.7 M. The temperature was 303 K. Lines are drawn only as visual aids.

N/O-states of H35 C2 and Y60 2,6 and 3,5 resonances also could be observed. These observations are consistent with the presence of slow NMR exchange between/among N- and O-states.

At lower 2-propanol concentrations, multiple O-state resonances are apparent. Two Y60 3,5 O-state resonances

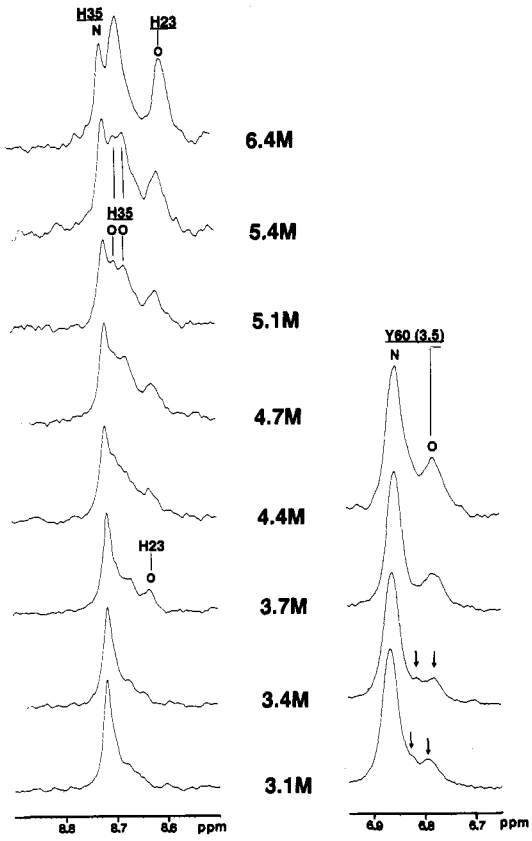

FIGURE 6: Multiple O-states of Y60 and H35. Expanded regions of 600-MHz NMR spectra are shown for Y60 (3,5) and H35 C2 resonances to indicate the presence of two O-states. The 2-propanol concentration is as indicated.

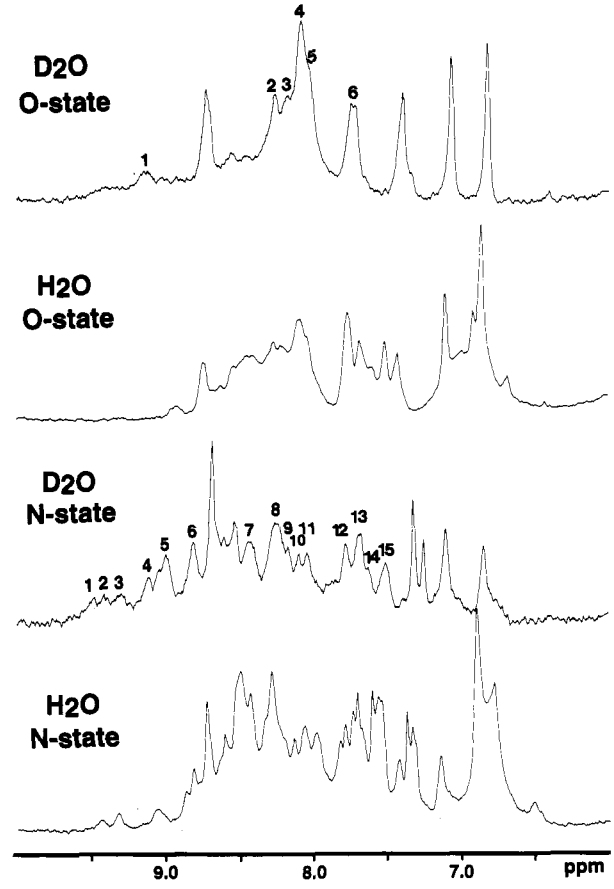

FIGURE 7: Backbone NH resonances in N- and O-states. ^1H_2O and ^2H_2O NMR proton spectra (600 MHz) are shown for PF4 in 3.3 M 2-propanol to indicate NH resonance dispersion for the N-state and in 9.8 M 2-propanol to indicate NH resonance shifts in the O-state. Solution conditions were pH 4, 303 K, and the protein concentration was 5 mg/mL. Comparative spectra are also shown in ^2H_2O to indicate the presence of long-lived backbone NHs. The pH in ^1H_2O and ^2H_2O solutions has not been corrected for isotope effects; therefore, differences in resonance chemical shifts can be noticed.

are observed at 3.1 and 3.4 M 2-propanol (Figure 6). This suggests that at least two stable O-states exist and that these are initially in slow exchange with native PF4 and with each other. Aside from increasing in intensity on increasing 2-propanol concentration, the two Y60 O-state resonances shift together and then coalesce apparently as exchange between/among O-states shifts from slow- to fast-exchange regime. At 4.7 M 2-propanol, two O-state H35 C2 resonances are also apparent. These are evidently present at lower 2-propanol concentrations, although they are not as resolved. In contrast to the two Y60 O-state resonances observed during the 2-propanol titration, H35 O-state resonances vary in intensity relative to each other with the more upfield of the two attaining a greater population prior to the minor resonance either fading away or shifting to under the major one.

O-State Structural Characterization. NMR data in Figure 2 suggest that the O-state is more "unfolded" or "open" relative to the N-state. Downfield-shifted αH resonances which are associated with anti-parallel β-sheet structure in PF4 (Barker and Mayo, unpublished results) are highly upfield-shifted and less dispersed as are backbone NH resonances (Figure 7). Upfield methyl resonances (Figure 3) also appear to be less dispersed in the O-state. Additionally, the highly elevated O-state H23 pK_a mentioned above is consistent with the idea of a less "folded" conformation.

Far-ultraviolet CD spectra of PF4 are shown in Figure 8 as a function of 2-propanol concentration. All traces show similar negative ellipticity distributions, consistent with CD spectra of structured proteins (Brahms & Brahms, 1980; Johnson, 1988, and references cited therein). Gaussian deconvolution and comparison with a data base of CD spectra on known protein structural compositions (Provencher & Glöckner, 1981; Provencher, 1982) yield distributions of percent α-helix, β-structure, and random coil [or better remainder (R)] as given in bar graph format in Figure 8 inset. Titrating with 2-propanol from 3.3 to 9.8 M decreases β-structure by about 30% and increases α-helix content by about 25%. Under conditions where O-state dominates, α-helix represents about 30–35% secondary structure, while β-structure represents about 20–25%. Consistent with the structural destabilizing effects of alcohols (Parodi et al., 1973), the "random coil" average fractional composition increases 10–15%. Reduction in β-sheet structure correlates with the observation of upfield-shifted, downfield αH resonances assigned to residues within the extensive anti-parallel β-sheet conformation in PF4. In native PF4, α-helix originates mostly from the C-terminal domain. The significant increase in α-helix composition is somewhat puzzling, but the ability of alcohols to stabilize helix structure (Conio et al., 1970) may account for this observation.

An apparent isodichroic point at about 200 nm suggests an equilibrium between two major conformational states, N-state and O-state. Although this may be somewhat surprising since NMR data mentioned earlier indicate the presence of multiple O-states at lower 2-propanol concentrations, the number of slowly exchanging O-states seems to be limited, and these tend to shift into one major O-state species as the alcohol concentration is increased. In addition, only one N-state is observed. If structural distributions between O-states are

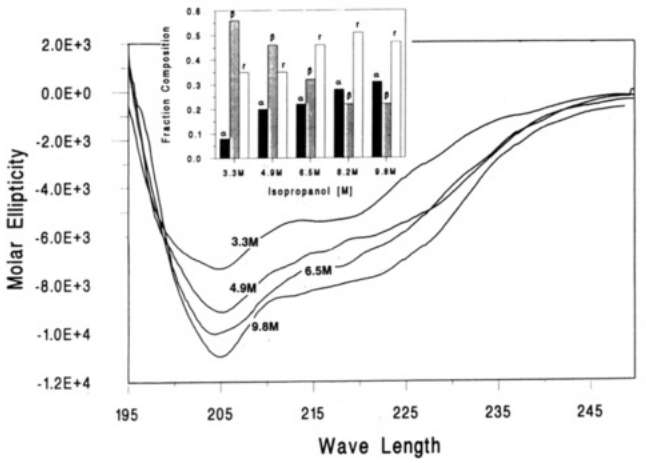

FIGURE 8: Far-ultraviolet CD spectra of PF4. Circular dichroic spectra for PF4 as a function of 2-propanol concentration are shown as mean residue ellipicity vs wavelength (nm). PF4 concentration is 17 μM in 10 mM phosphate buffer. The 2-propanol concentration is as indicated in the figure. The pH was adjusted to pH 4 as used for NMR titration data of Figure 2. The temperature was likewise controlled at 303 K. Other experimental variables are given under Materials and Methods.

generally the same, the presence of multiple O-states would not contradict the appearance of an isodichroic point.

Due to the presence of only one tyrosine, i.e., Y60, and no tryptophan or phenylalanine residues, the near-UV CD region (260–310 nm) was limited in information regarding tertiary structural differences (Baum et al., 1989) between N- and O-states. At 3.3 M 2-propanol, this CD spectral region (data not shown) yields a rather broad, nearly flat negative band from 265 to 290 nm, which becomes more positive on going up to 310 nm. At 9.8 M 2-propanol, this negative ellipicity remains. Addition of 8 M guanidine hydrochloride shifts that negative ellipicity toward zero. This suggests that the O-state possesses at least some tertiary structure. From this information alone, however, it is difficult to conclude whether or not appreciable change in PF4 tertiary structure has occurred in the O-state. Major shifts in secondary structure and reduction in β-sheet structure judged by both CD and NMR suggest that the tertiary structure has been modified by titration with 2-propanol.

Under conditions where PF4 is mostly in the O-state, long-lived backbone amide proton/deuteron exchange rates (Table I) support the idea of "folded" structure in the O-state. Initial NMR exchange spectra indicate that about 20–25 backbone NH protons (estimated from relative integrated area) are still present within 20 min after PF4 is dissolved in deuterium oxide/9.8 M 2-propanol, pH 3.2 and 25 °C, while 30–35 NHs are initially present in 3.3 M 2-propanol under otherwise equivalent conditions. A number of these NHs exchange rapidly and may be attributable to H/D exchange within solvent-exposed, random coil structure, i.e., equivalent to intrinsic exchange defined by Englander and Poulsen (1969). The intrinsic H/D exchange rate under these experimental conditions is estimated to be 20×10^{-4} s^{-1} by the Englander and Poulsen (1969) empirical equation for solvent-accessible amide protons in model peptides. Decay curves for some NH resonance envelopes are multiphasic (data not shown), and only estimates of exchange rate constants can be had from extreme slopes of these curves. These values are given in Table I for NH resonances labeled in Figure 7. Some 12–15 backbone amides exchange 7–36 times slower than the random coil rate and can be considered relatively long-lived. For comparison, exchange rates in the N-state have also been

Table I: Amide Exchange Rates for N-State and O-State PF4 at pH 3.5 and 25 °C

O-state PF4		N-state PF4	
resonance no.[a]	apparent exchange rate ($\times 10^5$ s^{-1})	resonance no.[a]	apparent exchange rate($\times 10^5$ s^{-1})
1	22 (1)[b]	1	4.6
2[c]	26 (1)[b] and 11 (1)[b]	2	6
3[c]	28 (1)[b] and 5.6 (1)[b]	3[c]	24 (1)[b] and 3.5 (1)[b]
4[c]	28 (4)[b] and 11 (2)[b]	4	1.5
5	26 (1)[b]	5[c]	9 (1)[b] and 1.6 (2)[b]
6	30 (2)[b]	6[c]	12 (1)[b] and 1.7 (1)[b]
		7	47 (2)[b]
		8[c]	36 (2)[b] and 7.8 (1)[b]
		9	10
		10	18
		11	15
		12	30
		13[c]	46 (1)[b] and 4 (1)[b]
		14	30
		15	42

[a] Arbitrary resonance numbers are given from downfield to upfield for resonances labeled in Figure 7. [b] An estimate of the number of exchanging amides in a given resonance envelope is given in parentheses. [c] These resonances for native PF4 show biphasic kinetic exchange curves; apparent exchange-rate constants have been estimated from initial and final slopes of these curves. All other resonances for native PF4 are apparently single resonances or at least exchange at nearly the same rate.

measured in the presence of 3.3 M 2-propanol. These also are listed in Table I for NH resonances labeled in Figure 7. Many of these long-lived N-state NHs are associated with protons in anti-parallel β-sheet structure (unpublished results). Interestingly, these N-state exchange rates, while normally slower, are similar to those found for the 12 or so long-lived NHs in O-state PF4 monomers (Table I), suggesting the presence of some structure folding in the O-state. It might also be added that, in the absence of 2-propanol, amide exchange rates for the N-state (Mayo et al., 1992) are by themselves considerably faster than those observed for what may be considered a "rigid" protein of comparable molecular weight where NH lifetimes can be measured in days or weeks. Qualitatively, this seems to suggest that even native PF4 monomers are relatively structurally flexible.

Two questions now arise: (1) is the effect of titrating from 3.3 (N-state) to 9.8 M (O-state) 2-propanol reversible and (2) are the NHs that exchange slowly in the O-state the same as those in the N-state? Both questions can be addressed by performing an alcohol-jump experiment. A 1-mL sample of PF4 (10 mg/mL) was made up on ice in 3.3 M 2-propanol at pH 3.2. Half the sample was held in a water bath at 25 °C at the same time that the other half was brought up to 9.8 M 2-propanol. NMR spectra were accumulated on the 9.8 M 2-propanol sample until about 50% of the long-lived amides had exchanged (about 60 min), at which time that sample was diluted 3-fold, making the 2-propanol concentration 3.3 M. NMR spectra were acquired on both (paired) 3.3 M 2-propanol samples. Results are displayed in Figure 9 along with the last spectrum of the 9.8 M 2-propanol sample prior to the alcohol-jump (bottom trace). These data show that the formation of the O-state is reversible and indicate that the O-state is a true PF4 folding intermediate.

The alcohol-jump experiment also indicates that the long-lived NHs in the O-state are mostly the same as those found in the N-state. Individual exchange rates, however, do vary. In particular, the most downfield-shifted NHs which are associated with residues involved in anti-parallel β-sheet in the N-state (see Figure 1) exchange more rapidly in the O-state. In fact, NH resonances 1, 2, and especially 6 exchange

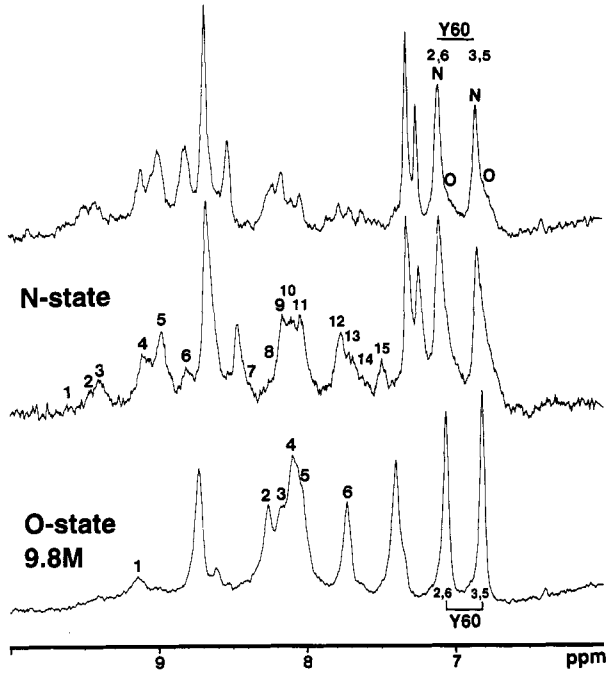

FIGURE 9: Alcohol-jump H/D exchange NMR spectra. The downfield aromatic and amide resonance regions are shown for three NMR spectra (600 MHz) as discussed in the text. The bottom trace is for PF4 (10 mg/mL) in the O-state (9.8 M 2-propanol) prior to the alcohol-jump to 3.3 M 2-propanol (3-fold dilution with ^2H_2O) (middle trace). The top trace shows the spectrum for a nearly equivalent time point for N-state PF4 that was kept at 3.3 M 2-propanol during the course of the alcohol-jump experiment (H/D exchange control spectrum). The pH was 3.2, and the temperature was 298 K.

10–15 times faster in the O-state, while NHs 3, 4, and 5 exchange only about 2–4 times faster. These differences have been estimated by knowing the exchange rates in 3.3 M 2-propanol (Table I) and comparing relative areas from the two parallel samples whose spectra are shown in Figure 9. This observation of increased NH exchange rates under otherwise constant conditions is consistent with CD and NMR results which indicate decreased β-sheet structure as 2-propanol concentration is increased. The fact that the same long-lived anti-parallel β-sheet NHs are still present in the O-state suggests that these structural elements are still present. Faster H/D exchange rates suggest a "loosening" of that tertiary structure.

More upfield NH resonances 10, 11, and especially 12 and 15 exchange more slowly by 2–4 times in the O-state. If the C-terminal helix were more stable in the O-state, some increased NH lifetimes might be expected. Further insight into this observation will have to await complete NH resonance assignments in the presence of 2-propanol.

At this point, one can summarize NMR and CD data by stating that the PF4 O-state possesses considerable secondary structure, but apparently lacks tertiary structural detail as observed for the N-state. These observations are consistent with the O-state being identified with some type of molten globule-like state.

If we are dealing with true equilibria between/among N- and O-states, then, for example, the conformation of the N-state should be generally maintained in the presence of 2-propanol. To address this, NOESY contour plots of the αH region are shown in Figure 10 for PF4 in 3.3 (A) and 5.7 M (B) 2-propanol. At 3.3 M 2-propanol, PF4 is over 90% N-state, while at 5.7 M 2-propanol, it stands at about 50% N-state and 50% O-state. This can be compared with similar

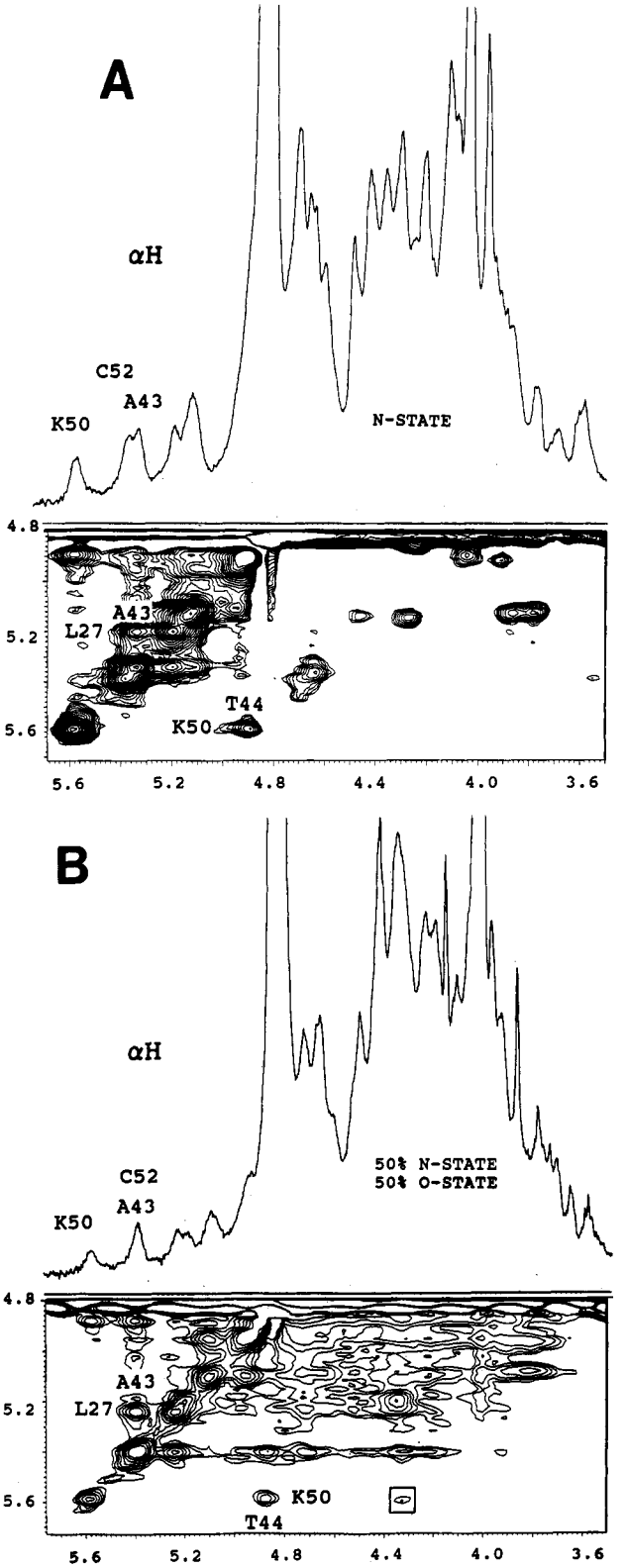

FIGURE 10: NOESY contour plots of αH–αH resonance region for PF4. The αH–αH resonance region of two 2D-NMR NOESY contout plots is shown for PF4 (pH 4, 303 K) in 3.3 and 5.7 M 2-propanol. The mixing time was 0.1 s. Other experimental details are given under Materials and Methods.

NOESY data accumulated on native PF4 in the absence of 2-propanol (Mayo et al., 1992). As mentioned earlier, NMR conformational analysis (results to be published elsewhere) indicates that these downfield-shifted N-state αH resonances result from anti-parallel β-sheet structure (Figure 1) (Mayo et al., 1992) as labeled in Figure 10. At either 3.3 or 5.7 M

2-propanol, although cross-peaks are somewhat chemically shifted, αH–αH NOESY connectivities characteristic of this structural motif are maintained. This indicates that the N-state PF4 anti-parallel β-sheet folding pattern is conserved even in the presence of up to 5.7 M 2-propanol.

These NOESY spectra give additional information concerning O-state resonance assignments and MT between N- and O-state resonances. As the 2-propanol concentration is increased (5.7 M 2-propanol), the O-state population increases. The NOESY spectrum in Figure 10B, therefore, appears to be a highly convoluted mix of NOE and exchange MT cross-peaks. At 3.3 M 2-propanol, where the O-state represents less than about 10% of the resonance intensity, chemical exchange cross-peaks are not apparent. Their presence at 5.7 M 2-propanol, however, severely limits our ability to resolve most NOE from exchange MT cross-peaks. The most downfield-shifted, N-state K50 αH resonance, however, is a single resonance that can be unambiguously traced to an N-state NOE with the opposing anti-parallel β-sheet T44 αH (Mayo et al., 1992) and to an apparent exchange MT cross-peak of the related O-state K50 αH resonance (tentative assignment; boxed-in in Figure 10B). The magnitude of this exchange MT cross-peak is much smaller than that noted earlier between N- and O-state H23 (and Y60) side-chain resonances. This is most likely due to a smaller αH resonance spin–lattice relaxation rate relative to those for H23 and Y60. Due to resonance overlap, possible multiple states, and 2-propanol-induced N-state chemical shifts, other O-state resonance assignments are presently not possible.

Transition Equilibria and Exchange Kinetics. This exceptional case of a stable intermediate protein folded state found in slow NMR chemical exchange with its native folded state provides a unique opportunity not only to deduce N-state/O-state equilibrium constants, called K_N and K_O according to the equilibrium

$$\text{N-state} \underset{k_N}{\overset{k_O}{\rightleftharpoons}} \text{O-state} \qquad (1)$$

where $K_N = 1/K_O = [N]/[O]$, but also to estimate exchange jump rates, i.e., k_O and k_N, or lifetimes of each state, from line widths which vary as a function of 2-propanol concentration. To avoid ambiguity and serious error, this analysis is limited to well-resolved resonances and, therefore, is focused on H23 C2, H35 C2, and Y60 3,5 side-chain ring proton resonances and on the K50 αH resonance. The K50 αH resonance is particularly important to this analysis for two reasons: (1) it represents a backbone proton which (2) is structurally positioned within the middle of the PF4 N-state anti-parallel β-sheet domain (see Figure 1). In this respect, possible arguments that observed spectral line-width effects could be the result of 2-propanol influencing protein side-chain conformations or hindered rotations as opposed to backbone folding transitions are countered. In addition, line-width changes discussed herein are independent of PF4 concentration (1 mg/mL to 10 mg/mL range), indicating that known PF4 aggregation does not play a role in this process.

As a function of 2-propanol concentration, the N-state fractional population is plotted in Figure 11A. For calculating K50 αH fractional populations, it was assumed that the resonance area for K50 αH in the N-state normalized to that of half the total Y60 3,5 resonance area was the fraction of K50 in the N-state. The difference from one, therefore, was the fraction of K50 in the O-state. At lower alcohol concentrations, N-state fractional populations are essentially equal for any probe site. This cannot be said at higher alcohol

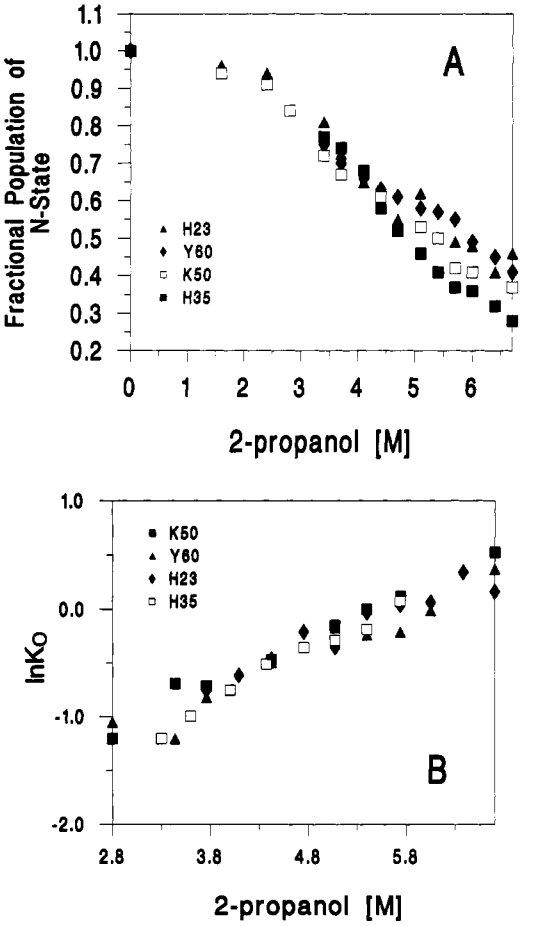

FIGURE 11: Effect of 2-propanol on N-state fractional population and equilibrium constants. Plots are shown for PF4 N-state fractional populations at H23, H35, Y60, and K50 probe sites (panel A) as well as for the O-state equilibrium constants, K_O (panel B), vs 2-propanol concentration. Values for the fractional populations and K_O were derived as discussed in the text.

concentrations where at least the H35 N-state fractional population drops faster than it does for the others. The Y60 N-state population apparently slopes the least. This suggests possible local effects on folding transitions. By 8 or 9 M 2-propanol, the N-state fraction has plateaued off at about 0.25 for H35 and 0.35 for the others. This indicates a limiting effect of 2-propanol on PF4 N-state/O-state equilibrium.

The natural logarithms of K_O for Y60, H35, H23, and K50 are plotted in Figure 11B. These have been calculated by taking the ratio of areas for respective N- and O-states identified in Figures 2 and 4. In cases where two O-states are observed, the ratio is taken with only one of these. As expected, K_O values increase with increasing 2-propanol concentration as observed in fractional populations shown in Figure 11A. K_O trends are similar for H23, H35, Y60, and K50, suggesting that one (or one type of) major folding process is occurring. This is consistent with CD data which show an apparent isodichroic point on titrating from 3.3 to 9.8 M 2-propanol. It does contrast, however, with fractional populations shown in Figure 11A. The reason for this is unclear.

In the present case of slow–intermediate NMR exchange, values for k_N and k_O exchange jump rates may be derived from resonance line widths (Jardetzky & Roberts, 1981) where resonances are broadened by an amount proportional to the rate of exchange or to the steady-state flux rate out of the state observed, i.e., inverse of the lifetime of that state. This

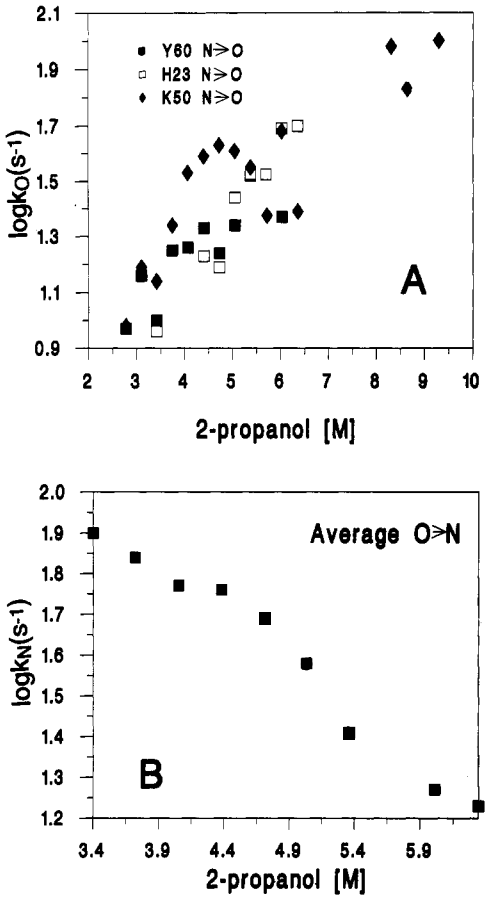

FIGURE 12: Jump rates between N- and O-states. Half-height line widths as derived from Lorentzian/Gaussian line fits discussed in the text were used to calculate k_O jump rates according to eq 2. Values for log k_O are plotted for H23, H35, Y60, and K50 probe sites as a function of 2-propanol concentration. k_N jump rates were estimated from k_O and K_O values as discussed in the text.

is expressed mathematically in

$$\pi(\Delta\upsilon^{N'}{}_{1/2} - \Delta\upsilon^{N}{}_{1/2}) = (P_O/P_N)k_N \qquad (2)$$

where $\Delta\upsilon^{N'}{}_{1/2}$ is the half-height line width of an N-state resonance in the presence of exchange and $\Delta\upsilon^{N}{}_{1/2}$ is its half-height line width in the absence of exchange. P stands for the population in either N- or O-states as denoted by subscripts. A similar expression can be written for line-width differences in the O-state.

As a function of 2-propanol concentration, log k_O (N → O) values from Y60 3,5, H23 C2, and K50 αH resonance line-width analyses are given in Figure 12A. Values for k_O range from 9 to 109 s^{-1} between 2.8 and 9 M 2-propanol. Given the experimental error, it is impossible to say if k_O values differ significantly from probe site to site. For jump rates out of the N-state, this analysis is valid since only one N-state resonance is observed. For jump rates out of the (an) O-state, the presence of two Y60 and H35 O-state resonances complicates any analysis and interpretation. In this respect, derived jump rates might be some weighted value of steady-state flux rates between/among N- and O-states. For this reason, average k_N values were estimated from derived k_O (Figure 12A) and K_O (Figure 11B) values ($K_O = k_O/k_N$). For each 2-propanol concentration, k_O and K_O values were first respectively averaged over all probe sites, and an average k_N value then was calculated from $k_N = k_O/K_O$. The natural logarithm of k_N is plotted in Figure 12B.

Since from 3 to 6 M 2-propanol the slope of log k_N appears to be linear, the protein folding rate in the absence of alcohol was estimated by simple linear extrapolation to 0 M 2-propanol. An apparent exchange rate, k_N, of about 500 s^{-1} was estimated. This corresponds to an O-state lifetime of about 2 ms and indicates that the time scale for the O-state to N-state transition is in the millisecond range. This in turn suggests that initial folding events for the unfolded, U-state, to O-state occur on a submillisecond time scale. H/D NMR trapping experiments (Roder et al., 1988) have already suggested that initial folding events occur on a time scale that is equal to or shorter than 5–10 ms. These data on PF4 are consistent with that observation.

DISCUSSION

Since folded protein structures are marginally stable at best, a delicate balance of forces dictates protein stability in solution. Addition of 2-propanol (or similar alcohols) to PF4 shifts the native conformation into an intermediate structural state. Here, this is referred to as the O-state for alcohol-induced structural state. O-States join the group of other types of stable intermediate structures such as A-states (*a*cid destabilized), D-states (urea or guanidine hydrochloride *d*enatured or *d*estabilized), and S-states (disulfide reduced). It is important to recognize that PF4 O-states may or may not play an active role in the actual folding process, and even though they may represent nonnative intermediates, the alcohol-induced folding transition in PF4 is reversible, implying that these O-states still represent true folding intermediates. The properties of partially organized protein states, in which only a subset of native folding interactions may be present, are of fundamental importance in relation to our understanding the nature of protein folding.

Relative to the PF4 N-state, the PF4 O-state displays a decrease in anti-parallel β-sheet structure which is apparently the result of alcohol-induced destabilization (Parodi et al., 1973; Conio et al., 1970). Interestingly, although β-structure is decreased as the concentration of 2-propanol is increased, α-helix structure is increased. It is not clear, however, whether this is the result of new helix formation or the stabilization of existing helix structure. Since alcohols are known to stabilize helix conformation in peptides (Conio et al., 1970, and references cited therein), it is likely that at least part of the observed increased α-helix content results from stabilization of the existing C-terminal helix segment. Both NMR and CD results agree that PF4 β-structure is generally decreased on titration with 2-propanol.

Long-lived NH resonances can be assigned tentatively as 1:A43, 2:T25, 3:I42,L45, 4:L27, 5:I51,L53, and 6:E28,T44 (Barker and Mayo, unpublished results). From Figure 1 it is apparent that this domain defines one segment of anti-parallel β-sheet structure in PF4. Alcohol-jump experiments indicate that long-lived NHs found within this anti-parallel β-sheet structure in native PF4 are generally perserved in the PF4 O-state but that they are in significantly faster exchange in the O-state. This suggests that the O-state maintains structural elements present in the N-state. Folded β-sheet structures, however, are probably more transient. The apparent increase in α-helix structure may explain some increased NH lifetimes. From H/D exchange experiments alone, this is difficult to say, however, since NMR studies on the molten globule state of α-lactalbumin, which has extensive secondary structure and a condensed hydrophobic core, show only a few NH groups that are highly protected against exchange (Doglikh et al., 1984; Dobson & Evans, 1988), whereas the NH groups in barnase are extensively protected (Matouschek et al., 1990; Bycroft et al., 1990). This must

await further in-depth structural analysis of the PF4 O-state, which is presently underway.

In some ways, the PF4 O-state resembles a molten globule intermediate (Ptitsyn, 1987; Kuwajima, 1989) whose structure is compact and has substantial secondary conformation but has few fixed, or perhaps more transient, tertiary interactions. Such intermediates are most often observed for proteins with a low overall stability where weak long-range folding interactions are "destabilized" under mildly "denaturing" conditions. For native PF4, low stability is suggested by the presence of relatively fast exchanging long-lived backbone NHs (Mayo et al., 1992). In the PF4 O-state, tertiary structural contacts are apparently less "fixed". Increased helical stability, however, appears to contradict the actual definition of a molten globule state.

Nakano and Fink (1990) have found that staphylococcal nuclease can be driven to a stable intermediate molten globule-like state under conditions of 70% methanol, pH 7, and low temperature. For the 76-residue protein ubiquitin, Harding et al. (1991) reported an A-state (pH 2) whose formation requires 60% methanol for stabilization of a molten globule intermediate state. In this respect, their (Harding et al., 1991) A-state was not a true A-state, since both alcohol and low pH were needed to induce the intermediate state. In any event, their observations are consistent with those reported here for the effect of 2-propanol (and other alcohols) on PF4. At pH 4–5, methanol has the same effect on PF4, but a concentration of about 10 times that of 2-propanol is required to induce 50% O-state formation under similar experimental conditions. In this respect, 2-propanol is a much more effective alcohol cosolvent for stabilization of the O-state at pHs between 4 and 5. The effectiveness of various alcohols in this regard has been presented by Yang et al. (1993).

Since simple aliphatic alcohols are known to destabilize globular proteins (Hermans, 1966; Timasheff & Inoue, 1968; Conio & Patrone, 1969; Conio et al., 1970; Parodi et al., 1973), some effect on PF4 structural stability was anticipated. What was unexpected was the observation of individual N- and O-state resonances which result from the rate of interconversion between these states being slow compared to the respective chemical shift time scales, i.e., slow chemical exchange regime. In fact, the accidental occurrence of these folding rates falling within the slow–intermediate 600-MHz ^{1}H NMR exchange regime allows estimation of N-state/O-state equilibrium constants and exchange rates. Alcohol-induced exchange rates range from about 5 to 100 s^{-1}. In the case of methanol-induced structural transitions in ubiquitin (Harding et al., 1991), apparent exchange rates fell in the NMR fast-exchange regime. Baum et al. (1989) found that at the midpoint of the urea-induced α-lactalbumin unfolding transition line broadening due to the presence of intermediate chemical exchange allowed estimation of N-state/A-state exchange rates on the order of 7 s^{-1}. At the midpoint of the PF4 N-state/O-state transition, this present study shows an exchange rate of about 25 s^{-1}. Considering the diversity of the systems, both proteins and conditions used, exchange rates are remarkably similar. The α-lactalbumin unfolding transition was thermally induced, while the PF4 O-state (molten globule) transition was chemically induced. Bycroft et al. (1990), using tryptophan fluorescence to monitor the fast kinetics of barnase refolding from urea solutions, suggest that a fast refolding phase could be resolved into two phases of rate constants 11–16 and 4.6 s^{-1}. It is interesting to speculate that these events may correspond to MG to N-state transitions in barnase. The dead time of their stopped-flow spectrophotometer (about 30 ms) precluded observation of faster folding steps, perhaps U-state to MG transitions.

The observation that folding equilibria and kinetic rate constants are observed to be nearly the same as measured by four site-specific probes, i.e., H23, H35, Y60, and K50, suggests that the folding process consists of a single or at least one major concerted transition. This addresses the question of folding cooperativity. CD data support the idea of equilibrium between two major states. The concept of one major concerted transition does not preclude the existence of a multistate mechanism. In fact, under certain solution conditions, at least two stable PF4 O-states are observed as reflected in H23 and Y60 resonance populations. Therefore, multistate transitions are occurring.

In any protein folding reaction, one must address the question of transitions from the unfolded state(s). This present study indicates that even in the presence of high concentrations of alcohol, a stable intermediate O-state is present. This in turn suggests that the equilibrium from unfolded U-state to intermediate O-state is highly shifted in favor of the intermediate and, therefore, that the rate for this transition must be relatively rapid, more rapid than the rate from O-state to N-state. By linear extrapolation to 0 M 2-propanol, estimation of PF4 N-state/O-state exchange rates in the absence of 2-propanol yields a value for the folding rate from the O-state of about 500 s^{-1} (2-ms time scale) and an unfolding rate to the O-state of about 2–4 s^{-1}. In this respect, unfolded PF4 states rapidly condense into the intermediate O-state, following which a slower, rate-limiting step leads to N-state formation. This is consistent with the idea that the slowest rate-limiting step of refolding appears to be close to the native state in terms of ordered structure (Segawa & Sugihara, 1984; Goldenberg & Creighton, 1985). The slow rate-limiting steps of folding are generally preceded by the rapid formation of folding intermediates. Aside from the well-known rate-limiting folding steps of *cis,trans*-proline isomerization and disulfide bond formation [see review by Jaenicke (1991)], slow reshuffling reactions of almost native-like intermediates apparently play a role in the folding process (Vaucheret et al., 1987). High-resolution NMR "trapping" experiments show that most of the peptide chain is involved in the formation of early intermediates and that secondary structure has already formed within milliseconds (Udgaonkar & Baldwin, 1988; Roder et al., 1988). Of significance here is the fact that PF4 N-state/O-state exchange rates fall within the millisecond folding time scale. H/D NMR trapping experiments (Udgaonkar & Baldwin, 1988; Roder et al., 1988) give a maximal time scale for initial folding reactions occurring within less than 5–10 ms. If PF4 folding rates occur within 2–4 ms, then the unfolding to intermediate-state transition must occur on a less-than-millisecond time scale.

CONCLUSIONS

Alcohols are highly effective at inducing stable PF4 folding intermediates (O-states). Exchange between PF4 N- and O-states is slow on the 600-MHz ^{1}H NMR time scale. This provides us with a unique, novel way to study protein folding equilibria and kinetics. The time scale of folding from the intermediate O-state to the N-state is about 2 ms. The equilibrium between unfolded, U-state, and O-state is highly shifted in favor of the O-state. Assuming linearity in folding events, this suggests that folding from U-state to O-state occurs on a much faster time scale. This, in turn, has implications for protein folding models.

REFERENCES

Barker, S., & Mayo, K. H. (1991) *J. Am. Chem. Soc. 113*, 8199–8203.

Baum, J., Dobson, C. M., Evans, P. A., & Hanley, C. (1989) *Biochemistry 28*, 7–13.

Bax, A., & Davis, D. G. (1985) *J. Magn. Reson. 65*, 355–360.

Brahms, S., & Brahms, J. (1980) *J. Mol. Biol. 138*, 149–178.

Bycroft, M., Matouschek, A., Kellis, J. T., Jr., Serrano, L., & Fersht, A. R. (1990) *Nature 346*, 488–490.

Chen, M.-J., & Mayo, K. H. (1991) *Biochemistry 30*, 6402–6411.

Conio, G., & Patrone, E. (1969) *Biopolymers 8*, 57–65.

Conio, G., Patrone, E., & Brighetti, S. (1970) *J. Biol. Chem. 245*, 3335–3340.

Deuel, T. F., Keim, P. S., Farmer, M., & Heinrikson, R. L. (1977) *Proc. Natl. Acad. Sci. U.S.A. 74*, 2256–2258.

Dobson, C. M., & Evans, P. A. (1988) *Nature 335*, 666–667.

Dolgikh, D. A., Gilmanshin, R. I., Brazhnikov, E. V., Bychkova, V. E., Semisotnov, G. V., Venyaminov, S. Y., & Ptitsyn, O. B. (1981) *FEBS Lett. 136*, 311–315.

Dolgikh, D. A., Kolomiets, A. P., Bolotina, I. A., & Ptitsyn, O. B. (1984) *FEBS Lett. 165*, 88–92.

Englander, S. W., & Poulsen, A. (1969) *Biopolymers 7*, 379–393.

Ewbank, J. L., & Creighton, T. E. (1991) *Nature 350*, 518–520.

Feng, Y., Wand, A. J., & Sligar, S. G. (1991) *Biochemistry 30*, 7711–7717.

Freire, E., Murphy, K. P., Sanchez-Ruiz, J. M., Galisteo, M. L., & Privalov, P. L. (1992) *Biochemistry 31*, 250–256.

Goldberg, M. E., Semisotnov, G. V., Friguet, B., Kuwajima, K., Ptitsyn, O. B., & Sugai, S. (1990) *FEBS Lett. 263*, 51–56.

Goldenberg, D. P., & Creighton, T. E. (1985) *Biopolymers 24*, 167–182.

Harding, M. M., Williams, D. H., & Woolfson, D. N. (1991) *Biochemistry 30*, 3120–3128.

Hermans, J., Jr. (1966) *J. Am. Chem. Soc. 88*, 2418–2425.

Holt, J. C., Harris, M. E., Holt, A., Lange, E., Henschen, A., & Niewiarowski, S. (1986) *Biochemistry 25*, 1988–1996.

Jaenicke, R. (1991) *Biochemistry 30*, 3147–3161.

Jardetzky, O., & Roberts, G. C. K. (1981) *NMR in Molecular Biology*, Academic Press, New York.

Jeener, J., Meier, B., Backman, P., & Ernst, R. R. (1979) *J. Chem. Phys. 71*, 4546–4550.

Jeng, M.-F., Englander, S. W., Elöve, G. A., Wand, A. J., & Roder, H. (1990) *Biochemistry 29*, 10433–10437.

Johnson, W. C., Jr. (1988) *Annu. Rev. Biophys. Biophys. Chem. 17*, 145–166.

Kuwajima, K. (1989) *Proteins 6*, 87–103.

Kuwajima, K., Mitani, M., & Sugai, S. (1989) *J. Mol. Biol. 206*, 547–561.

Loscalzo, J., Melnick, B., & Handin, R. I. (1985) *Arch. Biochem. Biophys. 240*, 446–455.

Lowry, O. H., Rosebrough, N. J., Fan, A. L., & Randall, R. J. (1951) *J. Biol. Chem. 193*, 265–270.

Lu, J., & Dahlquist, F. W. (1992) *Biochemistry 31*, 4749–4756.

Matouschek, A., Kellis, J. T., Jr., Serrano, L., Bycroft, M., & Fersht, A. R. (1990) *Nature 346*, 440–445.

Mayo, K. H., & Chen, M. J. (1989) *Biochemistry 28*, 9469–9478.

Mayo, K. H., Barker, S., Kuranda, M. J., Hunt, A. J., Myers, J. A., & Maione, T. E. (1992) *Biochemistry 31*, 12255–12265.

Nakano, T., & Fink, A. L. (1990) *J. Biol. Chem. 265*, 12356–12362.

Ohgushi, M., & Wada, A. (1983) *FEBS Lett. 164*, 21–24.

Palleros, D. R., Reid, K. L., McCarty, J. S., Walker, G. C., & Fink, A. L. (1992) *J. Biol. Chem. 267*, 5279–5285.

Parodi, R. M., Bianchi, E., & Ciferri, A. (1973) *J. Biol. Chem. 248*, 4047–4051.

Provencher, S. W. (1982) *Comp. Phys. Commun. 27*, 229–242.

Provencher, S. W., & Glöckner, J. (1981) *Biochemistry 20*, 33–37.

Ptitsyn, O. B. (1987) *J. Protein Chem. 6*, 273–293.

Radford, S. E., Woolfson, D. N., Martin, S. R., Lowe, G., & Dobson, C. M. (1991) *Biochem. J. 273*, 211–217.

Roder, H., Elöve, G. A., & Englander, S. W. (1988) *Nature 335*, 700–704.

Rucinski, B. S., Niewiarowski, S., James, P., Walz, D. A., & Budzynski, A. Z. (1979) *Blood 53*, 47–62.

Segawa, S.-I., & Sugihara, M. (1984) *Biopolymers 23*, 2473–2488.

Shortle, D., Stites, W. E., & Meeker, A. K. (1990) *Biochemistry 29*, 8033–8041.

States, D. J., Haberkorn, R. A., & Ruben, D. J. (1982) *J. Magn. Reson. 48*, 286–293.

St. Charles, R., Walz, D. A., & Edwards, B. F. P. (1989) *J. Biol. Chem. 264*, 2092–2099.

Timasheff, S. N., & Inoue, H. (1968) *Biochemistry 7*, 2501–2508.

Udgaonkar, J. B., & Baldwin, R. L. (1988) *Nature 335*, 694–699.

Vaucheret, H., Signon, L., Le Bras, G., & Garel, J. R. (1987) *Biochemistry 26*, 2785–2790.

Waddell, W. J. (1956) *J. Lab. Clin. Med. 48*, 311–314.

Wider, G., Macura, S., Anil-Kumar, Ernst, R. R., & Wüthrich, K. (1984) *J. Magn. Reson. 56*, 207–234.

Yang, Y., Barker, S., Chen, M.-J., & Mayo, K. H. (1993) *J. Biol. Chem.* (in press).